Neutrinos and duality

O. Lalakulich, Ch. Praet, N. Jachowicz, J. Ryckebusch, T. Leitner, O. Buss, and U. Mosel

Citation: AIP Conference Proceedings **1189**, 276 (2009); doi: 10.1063/1.3274170
View online: http://dx.doi.org/10.1063/1.3274170
View Table of Contents: http://scitation.aip.org/content/aip/proceeding/aipcp/1189?ver=pdfcov
Published by the AIP Publishing

Neutrinos and duality

O. Lalakulich*, Ch. Praet†, N. Jachowicz†, J. Ryckebusch†, T. Leitner*, O. Buss* and U. Mosel*

*Institut für Theoretische Physik, Universität Giessen, Giessen, Germany
†Department of Subatomic and Radiation Physics, Ghent University, Ghent, Belgium

Abstract. A phenomenological study of Bloom-Gilman duality is performed in electron and neutrino scattering on nuclei. In the resonance region the structure functions are calculated within the phenomenological models of Ghent and Giessen groups, where only the resonance contribution is taken into account, and the background one is neglected. Structure functions F_2 in the resonance region are compared with the DIS ones, extracted directly from the experimental data. The results show, that within the models considered the Bloom-Gilman duality does not work well for nuclei: the integrated strength in the resonance region is considerably lower than in the DIS one.

Keywords: baryon resonance, neutrinoproduction, Bloom-Gilman duality, quark–hadron duality, structure function
PACS: 25.30.Pt, 13.15.+g, 14.20.Gk, 24.85.+p

INTRODUCTION

Nearly forty years ago, Bloom and Gilman found [1] that in electron scattering on protons the inclusive structure function F_2 in the resonance region oscillates around the DIS scaling curve and, after averaging, closely resembles it. Recent electron scattering measurements at Jefferson Laboratory (JLab) have confirmed the validity of the Bloom–Gilman duality for proton, deuterium [2] and iron [3] structure functions. If duality is understood quantitatively, there may be various applications. For example, the region of high Bjorken variable x is hardly experimentally investigated, because in the DIS region it would require very high Q^2 and thus huge luminosities. If duality is satisfied with good accuracy, one would be able to use the data in the resonance region to reach high x at reasonable Q^2.

The topic becomes even more interesting when turning to nuclear targets and neutrino sources. The current precision measurements of the oscillation parameters require an efficient and accurate description of the neutrino–nucleus cross sections. Of particular interest is the resonance region and the possibility of linking it with the DIS region. A hadronic description of a neutrino-nucleus cross section at low Q^2 requires the good knowledge of vector and axial transition form factors for each resonance. For the majority of the resonances, these transition form factors are not well constrained. Provided that one can establish that quark-hadron duality holds with a reasonable accuracy, one could think of using the DIS results for estimating the neutrino-nucleus cross sections in the transition region.

NUCLEONS

Starting from the pioneering work of Bloom and Gilman, the observation of duality in lepton scattering includes three features:

(i) the resonance region data oscillate around the scaling DIS curve
(ii) the resonance data are on average equivalent to the DIS curve
(iii) the resonance region data "slide" along the DIS curve with increasing Q^2.

So far, most theoretical studies of quark–hadron duality in lepton scattering were dealing with nucleon targets [4, 5, 6]. The DIS parts were considered as known, the structure functions in the scaling region being conventionally evaluated from leading twist (LT) parton distribution functions (PDF): for example, $F_2^{eN(LT)} = (F_2^{ep} + F_2^{en})/2 = 5x/18 \cdot (u + \bar{u} + d + \bar{d} + 2s/5 + 2\bar{s}/5)$, $F_2^{\nu N(LT)} = (F_2^{\nu p} + F_2^{\nu n})/2 = x(u + \bar{u} + d + \bar{d} + s + \bar{s})$. For nucleons, several parameterizations of the PDFs are generally available (from the GRV, CTEQ and MRST groups). In the region of moderate x, which is of interest for our duality study, they provide nearly the same results.

CP1189, *From Sixth International Workshop on Neutrino-Nucleus Interactions in the Few-GeV Region*,
edited by F. Sanchez, M. Sorel, L. Alvarez-Ruso, A. Cervera, and M. Vicente-Vacas

The studies of the resonance region differ in the way the models treat the resonant contributions and the way they extract the structure functions.

Notice, that the property (iii) of the above list can be observed, if a few [6] or even only one [4] resonance are taken into consideration. The advantage of the model [6] is that the structure functions are given as simple analytical functions of the momentum transfer squared Q^2 and the energy transfer ν, provided that the resonance form factors are known. In this work the first four resonances were considered. Generally, however, as it was argued by Close [7, 8], inclusion of several resonances of different parities is desirable.

The model of Rein-Sehgal, implemented by the Wroclaw group [5], includes 18 resonances and is applied for neutrinoproduction, but not for electroproduction.

Within the Giessen BUU (GiBUU) framework, 13 resonances can be considered for both electron and neutrino reactions. GiBUU is a Boltzmann–Uehling–Uhlenbeck transport model for nuclear reactions, developed by the Giessen theory group over the last two decades. Besides its original application to heavy ion collisions, the model is also successful in describing photon–, pion–, and electron–induced reactions, as well as neutrino–induced reactions in the resonance region. In April 2008, the GiBUU model source code has been published under GNU General Public License for public use [9].

In general, the GiBUU model is able to include all possible resonances provided that the form factors are available. Currently the electromagnetic form factors are taken from the MAID analysis [10, 11, 12]. In this analysis, 13 resonances with invariant masses of less than 2 GeV are included and this predefines our choice of the resonances. Besides resonance contributions, the model includes non-resonance background as described in Ref. [13].

Within the GiBUU code the cross section is calculated numerically and the structure functions $F_2 = \nu W_2$ is extracted from the cross section in a convenient way:

$$\frac{d\sigma^N}{dQ^2 d\nu} = k_{EM,CC} W_2(Q^2,\nu) \frac{\pi}{EE'} \left[1 - \frac{Q^2}{4EE'} + 2\frac{Q^2}{4EE'} \frac{Q^2\nu^2 + Q^4}{Q^4(1+R)} \right] \tag{1}$$

The ratio R, defined as $2xF_1(1+R) = F_2(1+4m_N^2x^2/Q^2)$, is the world average value

$$R(Q^2,x) = \frac{0.0635}{\ln(Q^2/0.04)} \left[1. + \frac{12.Q^2}{Q^2+1.0} \frac{0.125^2}{0.125^2+x^2} \right] + \frac{0.5747}{Q^2} - \frac{0.3534}{Q^4+0.09},$$

taken from [14]. The coefficients

$$k_{EM} = \frac{4\alpha_{em}^2 E'^2}{Q^4}, \qquad k_{CC} = \frac{G_F^2 E'^2}{2\pi^2},$$

are the Mott cross sections for electron and neutrino reactions. For electroproduction on an isoscalar target, $\sigma^N = (\sigma^{ep} + \sigma^{en})/2$ is half sum of electroproduction cross sections on proton and neutron. For charged current neutrinoproduction, in order to eliminate the structure function F_3, one should use the linear combination of the neutrino and antineutrino cross sections. For an isoscalar target it is sufficient to take

$$\sigma^N = (\sigma^{\nu p} + \sigma^{\bar{\nu} p} + \sigma^{\nu n} + \sigma^{\bar{\nu} n})/4\,. \tag{2}$$

For a quantitative estimate of the validity of duality it is convenient to introduce the ratio of the integrals of the resonance (res) and DIS structure functions

$$I_i(Q^2) = \frac{\int_{\xi_{\min}}^{\xi_{\max}} d\xi\ \mathscr{F}_i^{(\mathrm{res})}(\xi,Q^2)}{\int_{\xi_{\min}}^{\xi_{\max}} d\xi\ \mathscr{F}_i^{(\mathrm{DIS})}(\xi,Q^2_{DIS})}\,, \tag{3}$$

where $\mathscr{F}_i$ denotes $2xF_1$, F_2 or xF_3 (for neutrino scattering). The value Q^2_{DIS} is taken as the actual Q^2 value for a given parameterization of DIS PDFs or DIS experimental data set. Under conditions of perfect quark–hadron duality this ratio would be 1 and independent of Q^2. Thus, the degree to which the local duality is fulfilled can be estimated from the Q^2 dependence and the deviation from 1 of the computed I_2.

Here we present our recent results for the nucleon, obtained within the GiBUU model. The isoscalar nucleon F_2^{eN} structure function, which includes both resonance and background contributions, is shown at the left panel of Fig. 1 versus the Nachtman variable ξ. Notice, that ξ decreases with increasing invariant mass W. For a given Q^2 value, the highest peak at the larger ξ value correspond to the $\Delta-$resonance peak, and the two lower peaks at smaller values of

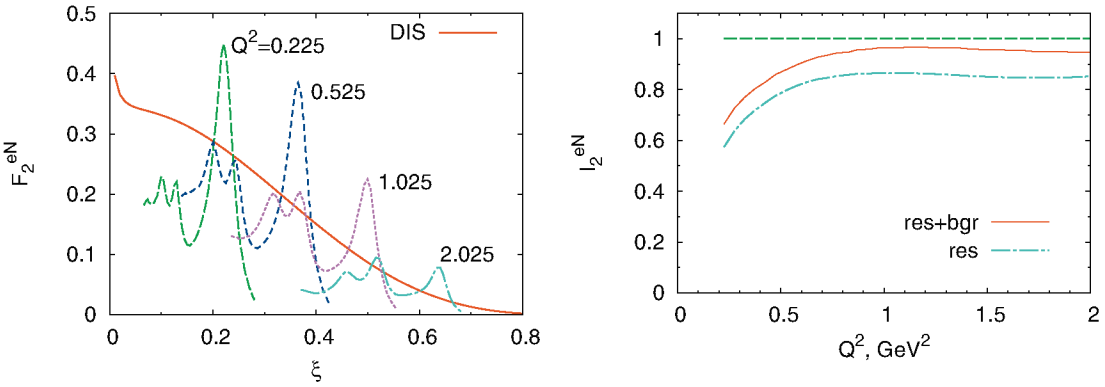

FIGURE 1. Duality for the isoscalar nucleon F_2^{eN} structure function calculated within GiBUU model. (Left) F_2^{eN} as a function of ξ, for $Q^2 = 0.225, 0.525, 1.025$ and 2.025 GeV^2 (indicated on the spectra), compared with the leading twist parameterizations at $Q^2 = 10$ GeV^2. (Right) Ratio I_2^{eN} of the integrated F_2^{eN} in the resonance region to the leading twist functions.

ξ correspond to the second ($1.40\,\text{GeV} \lesssim W \lesssim 1.56\,\text{GeV}$) and the third ($1.56\,\text{GeV} \lesssim W \lesssim 2.0\,\text{GeV}$) resonance regions. The general picture shows a reasonable agreement with the duality hypothesis.

In the right panel of Fig. 1, the ratio of the integrals I_2^{eN}, defined in (3), is shown not only for the whole structure function (resonance + 1-pion background), but also for the resonance contribution separately.

For $Q^2 > 0.5$ GeV^2, the ratio I_2^{eN} for the resonance contribution only is at the level of 0.85, which is smaller and flatter in Q^2 in comparison with the results [6, 15] of the Dortmund group resonance model. The difference is due to the different parameterization of the electromagnetic resonance form factors used in the two models. The background gives a noticeable contribution and brings the ratio up to 0.95. The fact, that it is smaller than 1 is of no surprise, because additional nonresonant contributions like 2- and many-pion background are possible, but not taken into account here. They are the subject of coming investigations.

The principal feature of neutrino reactions, stemming from fundamental isospin arguments, is that duality does not hold for proton and neutron targets separately. The interplay between the resonances of different isospins allows for duality to hold with reasonable accuracy for the average over the proton and neutron targets. We expect a similar picture emerges in neutrino reactions with nuclei.

For neutrinoproduction, the structure function $F_2^{\nu N}$ and the ratio $I_2^{\nu N}$ are shown in Fig. 2 for the resonance contribution only. The ratio is at the level of 0.7, which is (similar to the electron case) smaller than 0.8, which has been calculated within the Dortmund resonance model [6, 15]. Thus, one would expect a large contribution from the background. The role of the background in neutrino channel is under investigation now.

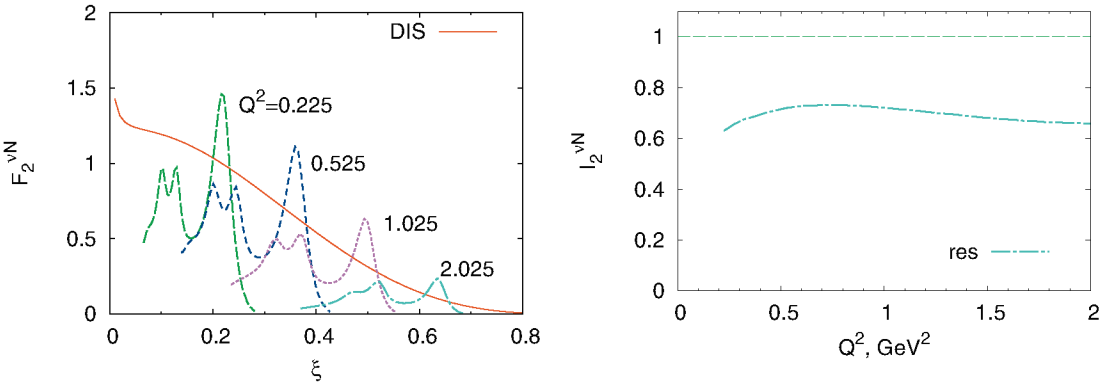

FIGURE 2. Duality for the isoscalar nucleon $F_2^{\nu N}$ structure function calculated within the GiBUU model. (Left) $F_2^{\nu N}$ as a function of ξ, for $Q^2 = 0.225, 0.525, 1.025$ and 2.025 GeV^2 (indicated on the spectra), compared with the leading twist parameterizations at $Q^2 = 10$ GeV^2. (Right) Ratio $I_2^{\nu N}$ of the integrated $F_2^{\nu N}$ in the resonance region to the leading twist functions.

Recent electron scattering measurements at JLab have confirmed the validity of the Bloom–Gilman duality for proton, deuterium [2] and iron [3] structure functions. Further experimental efforts are required for neutrino scattering. Among the upcoming neutrino experiments, Minerνa[16, 17, 18] and SciBooNE[19, 20, 21] aim at measurements with carbon, iron and lead nuclei as targets.

One of the major issues for nuclear targets is the definition of the nuclear structure functions $F^A_{1(2,3)}$. Experimentally they are determined from the corresponding cross sections, using Eq. (1).

We follow the same procedure, using the GiBUU cross sections. So, at the first step the inclusive double differential cross section $d\sigma/dQ^2d\nu$ is calculated within the GiBUU model. The nucleon is bound in a mean field potential, which is parameterized as a sum of a Skyrme term term depending only on density and a momentum-dependent contribution of Yukawa-type interaction. Fermi motion of the bound nucleon and Pauli blocking are also considered (see [13] for details).

Previous work [22] has used the analytical formulas for the nucleon structure functions, presented in [6], and directly apply nuclear effects to them. Nuclear effects are treated within the independent particle shell model, so that each bound nucleon in a nucleus occupies a nuclear shell α with a characteristic binding energy e_α and is described by the bound–state spinor u_α. The four–momentum of the bound nucleon can be written as $p^\mu = (m_N - e_\alpha, \vec{p})$, thus the nucleon is off its mass shell. Both the bound–state spinor $u_\alpha(\vec{p})$ and the corresponding binding energies are computed in the Hartree approximation to the $\sigma - \omega$ Walecka–Serot model.

As shown in [22], this leads to the following definition of the nuclear structure functions

$$\mathscr{W}_2^A(Q^2,\nu) = \sum_\alpha \int d^3p\,(2j_\alpha+1)n_\alpha(p)\mathscr{W}_2(Q^2,\nu,p^2)\left[\frac{|\vec{p}|^2-p_z^2}{m_N^2}\frac{Q^2}{q_z^2} + \left(\frac{(p\cdot q)}{m_N\nu}\right)^2\left(1+\frac{p_z}{q_z}\frac{Q^2}{(p\cdot q)}\right)^2\right]. \quad (4)$$

In Fig. 3, the results of Ghent and Giessen models for the resonance contribution to the F_2^A/A structure functions for a carbon target are shown for several Q^2 values. They are compared to experimental data obtained by the BCDMS collaboration [23, 24] in muon–carbon scattering in the DIS region ($Q^2 \sim 30-50\,\mathrm{GeV}^2$). They are shown as experimental points connected by smooth curves. For different Q^2 values, the experimental curves agree within 5% in most of the ξ region, as expected from Bjorken scaling.

When investigating duality for a free nucleon, we took the average over free proton and neutron targets, thus considering the isoscalar structure function. Since the carbon nucleus contains an equal number of protons and neutrons, averaging over isospin is performed automatically. Due to the Fermi motion of the target nucleons, the peaks from the various resonance regions, which were clearly seen for the nucleon target, are hardly distinguishable for the carbon nucleus. In general, the curves of the Giessen model are above those of the Gent model, especially (as it would be natural to expect) in the second and the third resonance regions.

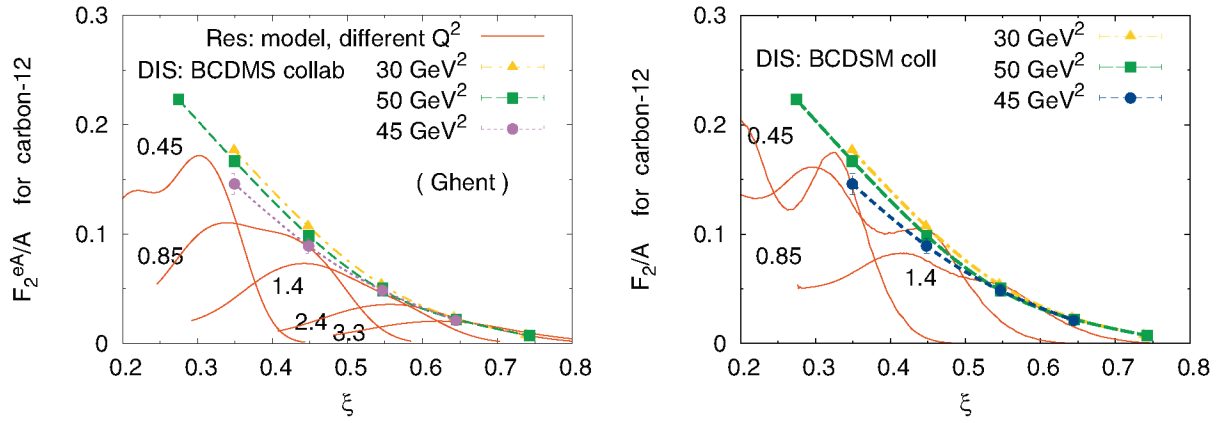

FIGURE 3. (Color online) Resonance curves $F_2^{e^{12}C}/12$ as a function of ξ, for $Q^2 = 0.45, 0.85, 1.4, 2.4$ and $3.3\ \mathrm{GeV}^2$ (indicated on the spectra), obtained within Ghent (left) and Giessen (right) models, compared with the experimental data [23, 24] in the DIS region at $Q^2_{DIS} = 30$, 45 and $50\ \mathrm{GeV}^2$.

As expected from local duality, the resonance structure functions for the various Q^2 values slide along a curve, whose ξ dependence is very similar to the scaling–limit DIS curve. However, for all ξ, the resonance curves lie below the experimental DIS data.

To quantify this underestimation, we now consider the ratio of the integrals of the resonance (res) and DIS structure functions, determined in Eq. (3) For electron–carbon scattering we choose the data set [24] at $Q^2_{DIS} = 50$ GeV^2, because it covers most of the ξ region. For nuclear structure functions, as it is explained in [22], the integration limits are to be determined in terms of the effective $\tilde{W}$ variable, experimentally (see, for example, [25]) defined as $\tilde{W}^2 = m_N^2 + 2m_N\nu - Q^2$. For a free nucleon $\tilde{W}$ coincides with the invariant mass W. For a nucleus, it differs from W due to the Fermi motion of bound nucleons, but still gives a reasonable estimation for the invariant mass region involved in the problem.

In particular, the resonance curves presented in all figures are plotted in the region from the pion–production threshold up to $\tilde{W} = 2$ GeV. For a free nucleon, the threshold value for 1-pion production (and thus the threshold value of the resonance region) is $\tilde{W}_{\rm min} = W_{\rm min} \approx 1.1$ GeV. Bound backward-moving nucleons in a nucleus allow lower W values beyond the free–nucleon limits. The threshold for the structure functions is now defined in terms of ν or $\tilde{W}$, rather than W. Hence, we consider two different cases in choosing the ξ integration limits for the ratio (3). First, for a given Q^2, we choose the ξ limits in the same manner as for a free nucleon:

$$\xi_{\rm min} = \xi(\tilde{W} = 1.6\,{\rm GeV}, Q^2), \qquad \xi_{\rm max} = \xi(\tilde{W} = 1.1\,{\rm GeV}, Q^2)\,. \tag{5}$$

We refer to this choice as integrating "from 1.1 GeV". The integration limits for the DIS curve always correspond to this choice. As a second choice, for each Q^2 we integrate the resonance curve from the threshold, that is from as low $\tilde{W}$ as achievable for the nucleus under consideration. This corresponds to the threshold value at higher ξ and is referred to as integrating "from threshold". With this choice we guarantee that the extended kinematical regions typical for resonance production from nuclei are taken into account. Since there is no natural threshold for the ξ_{min}, for both choices it is determined from $\tilde{W} = 1.6$ GeV, as defined in Eq. (5).

The results for the ratio (3) are shown in Fig. 4. The curve for the isoscalar free-nucleon case is the same as in Ref. [6] with the "GRV" parameterization for the DIS structure function. One can see that the carbon curve obtained by integrating "from threshold" lies above the one obtained by integrating "from 1.1 GeV", the difference increasing with Q^2. This indicates that the threshold region becomes more and more significant, as one can see from Fig. 4. Recall, that the flatter the curve is and the closer it gets to 1, the higher the accuracy of local duality would be.

Our calculations for carbon show that in the Ghent model the ratio is slightly lower than the free-nucleon value for both choices of the integration limits. In the Giessen model, the carbon ratio is at the same level as the free nucleon one or even higher. This is mainly due to the fact, that in Giessen model the structure function in second resonance region gets contributions from the 9 resonances, which were not present in Ghent model.

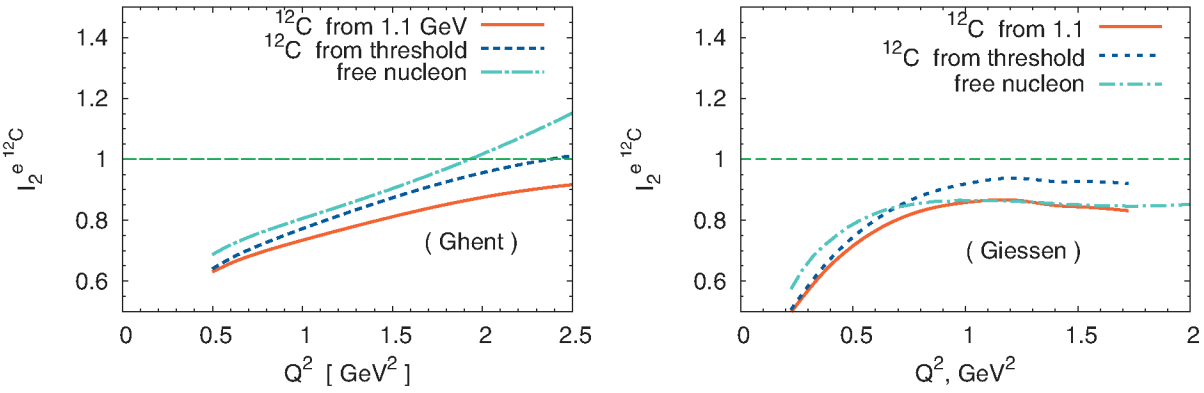

FIGURE 4. (Color online) Ratio defined in Eq.(3) for the free nucleon (dash-dotted line), and ^{12}C in Ghent (left) and Giessen (right) models. We consider the under limits determined by $\tilde{W} = 1.1$ GeV (solid line) and by the threshold value (dotted line).

For neutrino–iron scattering, the structure functions $F_2^{\nu Fe}$ are shown in Fig. 5. As for the electron-carbon results of Fig. 3, the resonance structure is hardly visible for both the Ghent and the Giessen model. The second resonance region is more pronounced in Giessen model because of the high mass resonances taken into account. The resonance structure functions are compared to the experimental data in DIS region obtained by the CCFR [26] and NuTeV [27]

collaborations. It appears, that the resonance curves slide along the DIS curve, as one would expect from local duality, but lie below the DIS measurements. Hence, the computed structure functions do not average to the DIS curve. The necessary condition for local duality to hold is thus not fulfilled.

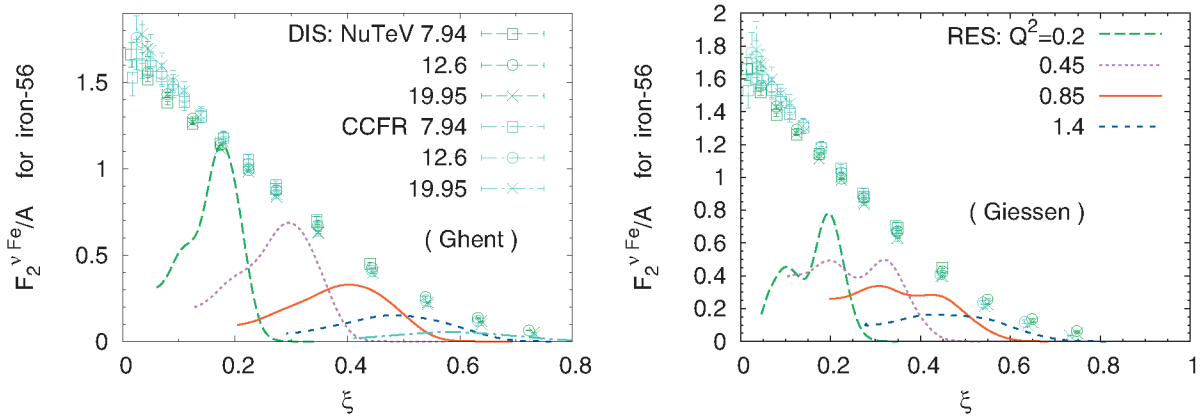

FIGURE 5. (color online) The computed resonance curves $F_2^{\nu\,^{56}Fe}/56$ as a function of ξ, calculated within Ghent(left) and Giessen (right) models for $Q^2 = 0.2, 0.45, 0.85$, 1.4, and 2.4 GeV^2. The calculations are compared with the DIS data from Refs. [26, 27]. The DIS data refer to measurements at $Q^2_{DIS} = 7.94$, 12.6 and 19.95 GeV^2.

The ratio $I_2^{\nu\,^{56}Fe}$ defined in Eq.(3) is shown in Fig. 6. The curve for the isoscalar free nucleon case is also presented for comparison. For the Ghent group plot it is identical to that presented in Ref. [6] with the "fast" fall–off of the axial form factors for the isospin-1/2 resonances. For the Giessen group plot it is identical to that in the right panel of Fig.1.

Our results show, that for both the Ghent and the Giessen models 1) this ratio is significantly smaller than 1 for all Q^2; 2) it is significantly smaller than the one for the free nucleon; 3) I_2 is even lower than the corresponding ratio for electroproduction; 4) I_2 slightly decreases with Q^2.

To summarize, within the two models, which implement elementary resonance vertices differently and treat nuclear effects differently, we obtain qualitatively the same effect, that the resonance structure functions are consistently smaller that DIS functions in the same region of Nachtmann variable ξ. This is not what one would expect from Bloom-Gilman duality. Recall, that in this analysis for nuclei, we included the resonance structure functions, and ignore the background ones. To estimate their contribution and compare the results with the nucleon case would be one of the primary tasks of coming investigation.

Further results of the Ghent model are given in [22].

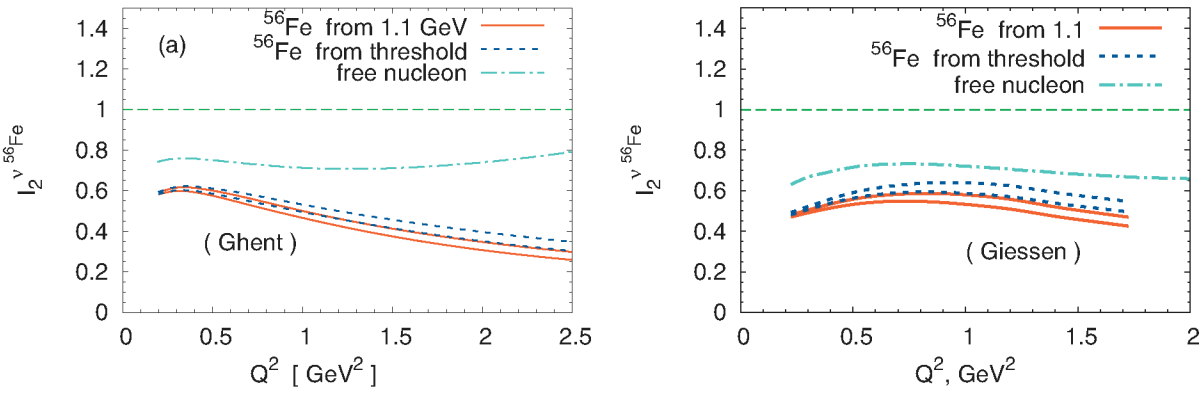

FIGURE 6. (color online) Ratio $I_2^{\nu\,^{56}Fe}$ defined in Eq. (3) for the free nucleon (dash-dotted line) and ^{56}Fe calculated within Ghent(left) and Giessen(right) models. For ^{56}Fe the results are displayed for two choices of the underlimit in the integral: $\tilde{W} = 1.1$ GeV (solid line) and threshold (dotted line). For each of these two choices we have used two sets of DIS data in determining the denominator of Eq. (3). These sets of DIS data are obtained at $Q^2_{DIS} = 12.59$ and 19.95 GeV^2.

ACKNOWLEDGMENTS

This work has been supported by the Deutsche Forschungsgemeinschaft (DFG). O.L. is also thankful to Deutsche Akademische Austauschdienst (DAAD) for the financial support of participation in the NuInt09 Workshop.

REFERENCES

1. E. D. Bloom, and F. J. Gilman, *Phys. Rev. Lett.* **25**, 1140 (1970).
2. I. Niculescu, et al., *Phys. Rev. Lett.* **85**, 1186–1189 (2000).
3. J. Arrington, R. Ent, C. E. Keppel, J. Mammei, and I. Niculescu, *Phys. Rev.* **C73**, 035205 (2006), nucl-ex/0307012.
4. K. Matsui, T. Sato, and T. S. H. Lee, *Phys. Rev.* **C72**, 025204 (2005), nucl-th/0504051.
5. K. M. Graczyk, C. Juszczak, and J. T. Sobczyk, *Nucl. Phys.* **A781**, 227–246 (2007), hep-ph/0512015.
6. O. Lalakulich, W. Melnitchouk, and E. A. Paschos, *Phys. Rev.* **C75**, 015202 (2007), hep-ph/0608058.
7. F. E. Close, and N. Isgur, *Phys. Lett.* **B509**, 81–86 (2001), hep-ph/0102067.
8. F. E. Close, and W. Melnitchouk, *Phys. Rev.* **C68**, 035210 (2003), hep-ph/0302013.
9. GiBUU, Gibuu website (2009), URL http://gibuu.physik.uni-giessen.de/GiBUU.
10. S. K. D. Drechsel, and L. Tiator, Maid website (2009), URL http://www.kph.uni-mainz.de/MAID.
11. L. Tiator, and S. Kamalov (2006), nucl-th/0603012.
12. D. Drechsel, S. S. Kamalov, and L. Tiator, *Eur. Phys. J.* **A34**, 69–97 (2007), 0710.0306.
13. T. Leitner, O. Buss, L. Alvarez-Ruso, and U. Mosel, *Phys. Rev.* **C79**, 034601 (2009), 0812.0587.
14. L. W. Whitlow, E. M. Riordan, S. Dasu, S. Rock, and A. Bodek, *Phys. Lett.* **B282**, 475–482 (1992).
15. O. Lalakulich, et al., *AIP Conf. Proc.* **967**, 243–248 (2007).
16. D. Boehnlein, *AIP Conf. Proc.* **967**, 304–306 (2007).
17. C. J. Solano Salinas, A. Chamorro, and C. Romero, *AIP Conf. Proc.* **947**, 239–244 (2007).
18. Minerνa collaboration homepage (2009), URL http://minerva.fnal.gov.
19. J. L. Alcaraz-Aunion, and J. Catala-Perez, *AIP Conf. Proc.* **967**, 307–309 (2007).
20. K. Hiraide, *AIP Conf. Proc.* **967**, 316–318 (2007).
21. Sciboone collaboration homepage (2009), URL http://www-sciboone.fnal.gov.
22. O. Lalakulich, N. Jachowicz, C. Praet, and J. Ryckebusch, *Phys. Rev.* **C79**, 015206 (2009), 0808.0085.
23. D. Bollini, et al., *Phys. Lett.* **B104**, 403 (1981).
24. A. C. Benvenuti, et al., *Phys. Lett.* **B195**, 91 (1987).
25. R. M. Sealock, et al., *Phys. Rev. Lett.* **62**, 1350–1353 (1989).
26. W. G. Seligman, et al., *Phys. Rev. Lett.* **79**, 1213–1216 (1997).
27. M. Tzanov, et al., *Phys. Rev.* **D74**, 012008 (2006), hep-ex/0509010.